

# Negative Poisson's ratios in few-layer orthorhombic arsenic from first-principles calculations

Jianwei Han, Jiafeng Xie, Z. Y. Zhang, D. Z. Yang, M. S. Si\*, and D. S. Xue†

*Key Laboratory for Magnetism and Magnetic Materials of the Ministry of Education,  
Lanzhou University, Lanzhou 730000, China*

(Dated: August 13, 2018)

## Abstract

A material exhibiting a negative Poisson's ratio is always one of the leading topics in materials science, which is due to the potential applications in those special areas such as defence and medicine. In this letter, we demonstrate a new material, few-layer orthorhombic arsenic, also possesses the negative Poisson's ratio. For monolayer arsenic, the negative Poisson's ratio is predicted to be around -0.09, originated from the hinge-like structure within the single layer of arsenic. When the layer increases, the negative Poisson's ratio becomes more negative and finally approaches the limit at four-layer, which is very close to the bulk's value of -0.12. The underlying mechanism is proposed for this layer-dependent negative Poisson's ratio, where the internal bond lengths as well as the normal Poisson's ratio within layer play a key role. The study like ours sheds new light on the physics of negative Poisson's ratio in those hinge-like nano-materials.

PACS numbers: 62.20.dj, 73.20.-r, 63.20.dk

Virtually all known materials would undergo a lateral contraction when stretched longitudinally and vice versa, which is protected by the conservation of volume under elastic loading. This gives a positive Poisson's ratio ( $\nu$ ). In isotropic materials, the positive Poisson's ratio is theoretically in the range from 0 (Cork) to 0.5 (Rubber) [1]. If a lateral dimension expands during stretching or vice versa, the exhibited Poisson's ratio is negative and the associated material is termed auxetic [2]. Much intense interest in this counterintuitive feature stems from the pioneering discoveries that critical fluids, re-entrant polymer foams, colloidal crystals, laser-cooled crystals, unscreened metals,  $\alpha$ -cristobalite, A7 structure elements arsenic and bismuth, and laminates are found to be auxetic [3–6]. Such an unusual mechanical property of  $\nu < 0$  makes a material possible for applications in those special areas. For example, compression in one direction results in a shrink not an expansion in the transverse direction, demonstrating the mechanism of bulletproof vests in national defence [7]; The opposite situation—an expansion responds to a stretch—is the manifestation of artificial limbs in medicine [8]. This sparks a surge in research activity in novel materials with negative Poisson's ratios.

In 2008, Hall and his colleagues found that negative Poisson's ratios can appear in low-dimensional carbon sheets when multiwalled nanotubes are introduced [9]. This is a big step towards the design of nanostructured composites, artificial muscles, gaskets, and chemical and mechanical sensors. Naturally, it raises a question whether the negative Poisson's ratio can emerge in other low-dimensional materials. In fact, it is difficult to measure this negative Poisson's ratio in experiments as the observation of such a ratio is spurious [10]. But, one can always predict it theoretically [11]. For example, monolayer of black phosphorus (BP) is reported to exhibit a negative Poisson's ratio through using *ab initio* method [12]. This negative Poisson's ratio is ascribed to the occurrence of hinge-like structure within a single layer of BP. Like BP, arsenic also possesses the hinge-like structures in the orthorhombic phase. More importantly, two groups independently demonstrate the thermal stability of its few-layer forms in this orthorhombic phase [13, 14]. Their bandgaps are both layer- and strain-dependent and the gap values are around 1 eV. More surprising is that the carrier mobility can approach as high as several thousand  $\text{cm}^2\text{V}^{-1}\text{s}^{-1}$  in these few-layer arsenic. All these make few-layer arsenic promising for future semiconducting applications. However, up to now, no study has been focused on the mechanical properties, in particular the negative Poisson's ratio. Thus, at present, it is timely to check the possible existence of negative

Poisson's ratios in few-layer orthorhombic arsenic.

In this Letter, the negative Poisson's ratio is reported to occur in few-layer arsenic through using first-principles calculations, which stems from the hinge-like structure within one single layer of arsenic. The negative Poisson's ratio is about -0.09 at monolayer. When layer increases, the negative Poisson's ratio becomes more negative and finally approaches the bulk's value of -0.12 at four-layer. This layer-dependent negative Poisson's ratio is demonstrated to closely follow the internal bond lengths, in particular the one perpendicular to the within layer direction, which indeed increase with layer. To better understand the underlying mechanism, a rigid mechanical model is proposed, shedding new light on the negative Poisson's ratio in those hinge-like vdW nano-materials.

First-principles calculations in this work are performed within the framework of density functional theory, as implemented in the SIESTA code [15]. We have used the generalized gradient approximation in the form of Perdew, Burke, and Ernzerhof functional [16]. The effect of van der Waals (vdW) interaction is taken into account by using the empirical correction scheme proposed by Cooper [17]. Only the valence electrons are considered in the calculation, with the core being replaced by norm-conserving scalar relativistic pseudopotentials [18] factorized in the Kleinman-Bylander form [19]. We have used a split-valence double- $\zeta$  basis set including polarization orbitals with an energy shift of 100 meV for all atoms [20]. The convergence is achieved when the difference of the total energies between two consecutive ionic steps is less than  $10^{-5}$  eV and the maximum force allowed on each atom is set to be 0.01 eV/Å.

We start our work from the orthorhombic bulk arsenic with space group  $Cmca$ , which is the same as BP. The conventional unit cell includes eight atoms, as shown in Fig. 1(a). Each As atom within a single layer is covalently bonded with three As atoms, forming a puckered graphene-like hexagonal structure. This puckered structure is also called a hinge-like structure, which consists of two orthogonal hinges (atoms 456 and 612). This sets up the basis for those exotic properties in few-layer arsenic. The lattice constants are optimized to  $a = 4.70$  Å,  $b = 3.77$  Å, and  $c = 11.11$  Å, generating the internal parameters  $r_{12} = 2.58$  Å,  $r_{34} = 2.56$  Å,  $\theta_{123} = 94.09^\circ$ , and  $\theta_{234} = 99.05^\circ$ . All these agree well with experimental and theoretical results [13, 21]. A primitive unit cell and its Wigner-Seitz cell are illustrated in Fig. 1(b). It is comprised of four inequivalent atoms, which is only one half of the bulk case. In principle, monolayer of arsenic (arsenene), as shown in Fig. 1(c), can be obtained through

exfoliating its bulk counterpart. Once it is formed, some changes occur. The corresponding lattice constants  $a$  and  $b$  are changed to be 4.73 Å and 3.71 Å, respectively. In comparison with its bulk phase,  $a$  increases while  $b$  decreases. This gives a direct effect on the internal parameters: bond lengths  $r_{12}$  and  $r_{34}$  are decreased to 2.53 Å and 2.50 Å, while the bond angle  $\theta_{123}$  is increased to 94.54° and leaves  $\theta_{234} = 100.36^\circ$  nearly unchanged. As the thermal stability of a material is important for real device applications, here we confirm it from the cohesive energy. The calculated cohesive energy of orthorhombic bulk arsenic is 2.90 eV/atom, which is smaller by 0.15 eV/atom than that of the A7 structure arsenic [22]. This coincides with the fact that the A7 structure is the favored phase in experiment. However, when they are isolated into monolayers, they become equally stable as the cohesive energy difference is only  $\sim 0.01$  eV/atom. This means monolayer of orthorhombic arsenic is possible in experiment.

The calculated band structure of bulk phase is displayed in Fig. 1(d). It clearly shows that the valence band maximum (VBM) and the conduction band minimum (CBM) locate at the same crystal momentum  $Z$  point, demonstrating a direct bandgap semiconductor with nearly zero gap value. However, when it goes into monolayer, it behaves as an indirect bandgap semiconductor, as shown in Fig. 1(e). This is because that VBM appears along the  $\Gamma$ - $X$  line and close to the  $X$  point, while CBM locates at the  $\Gamma$  point. The obtained bandgap is about 1 eV. The underlying mechanism of the bandgap transition from direct (bulk) to indirect (monolayer) is dominated by the mutual competition of the two interlayer bondings  $r_{12}$  and  $r_{34}$ , see also the discussion in our previous work [13]. In the following, we pay attention on the mechanical properties of few-layer arsenic.

When deformation is applied along the  $x$  direction, the responding strain in the  $y$  direction is shown in Fig. 2(a). Note that the positive (or negative)  $\varepsilon$  means a tensile (or compressive) strain. The obtained data (solid circles) behaves as a strongly nonlinear feature, which is well fitted by function of  $y = -\nu_1 x + \nu_2 x^2 + \nu_3 x^3$ . The linear parameter  $\nu_1$  is fitted to be 0.35 and can be regarded as the linear Poisson's ratio. Similarly, we can obtain the linear Poisson's ratio in the  $z$  direction, as shown in Fig. 2(b). The corresponding linear Poisson ratio is  $\nu = \nu_1 = 0.13$ , which is nearly twice that in the  $y$  direction. This means that  $z$  direction is harder than  $y$  direction when they respond to the strain applied along the  $x$  direction. It should be noticed that in the hinge-like structure of arsenic (see Fig. 1(a)), the deformation of  $z$  direction is dominated by the bond length  $r_{34}$  and the bond angle  $\theta_{234}$ ,

while that of  $y$  direction needs the changes of  $r_{12}$  and  $\theta_{123}$ . Perturbed by the same external field, such as the strain in our case, the bond angle is more easily affected than that of bond length. Thus, we can infer that the bond angle  $\theta_{123}$ , in comparison with  $\theta_{234}$ , are largely changed when the deformation is applied along the  $x$  direction. This coincides with our first-principle calculations.

If the deformation is applied along the  $y$  direction, the situation dramatically changes. In Fig. 2(c),  $\varepsilon_x$  linearly depends on  $\varepsilon_y$ . The fitted Poisson's ratio is  $\nu = 1.07$ , which is much larger than the Poisson's ratios when the deformation is applied along the  $x$  direction. This is the direct manifestation of anisotropic feature in mechanical properties, which is also the origin of anisotropic transport reported in our previous work [13]. Up to now, all the obtained Poisson's ratios are normal and positive. However, when we check the strain along the  $z$  direction responding to the  $y$ -direction loading, the law behaved as in Fig. 2(d) is opposite.  $\varepsilon_z$  increases with  $\varepsilon_y$ , leading to an unusual Poisson's ratio, namely  $\nu < 0$ . The fitted linear Poisson's ratio is  $\nu = -0.093$ . Its magnitude is very huge if one remembers the negative Poisson's ratio of around -0.027 in monolayer of BP [12]. This makes monolayer arsenic more suitable for applications in those special areas such as aerospace and defence where large negative Poisson's ratios are requested. For monolayer arsenic, the internal bond lengths are larger than those of 2.42 Å and 2.38 Å in monolayer BP [12]. In principle, under the same loading, larger bonding would bear a stronger deformation. This explains why monolayer arsenic holds a larger (more) negative Poisson's ratio, being consistent with that  $\nu$  mostly increases with atomic number  $Z$  [3].

It is well known that layer stacking is emerging as a new degree of freedom to tune the electronic properties of vdW hetero-materials [23]. However, its impact on the negative Poisson's ratio is still missing. In the following, we will demonstrate how it affects the negative Poisson's ratios in few-layer arsenic. Once an additional layer is added, the negative Poisson's ratio is changed accordingly as the effect of layer stacking is involved, as displayed in Fig. 3(a). In comparison with monolayer, the nonlinear feature of  $\varepsilon_z$  versus  $\varepsilon_y$  is significantly enhanced for bilayer. This is represented by the larger fitted parameters of cubic terms, which are at least twice that of monolayer. In the vicinity of zero,  $L_1$  and  $L_2$  are nearly identical. When the strain is beyond around  $\pm 4\%$ ,  $L_1$  and  $L_2$  largely separate from each other. This is because the two layers are no longer equivalent in bilayer due to the  $AB$  stacking. The separated feature in the stress-strain curves under larger strain reflects

the asymmetric structure of layers, confirming the validity of our simulations. The linear Poisson's ratio is fitted to be about -0.14, which is increased by  $\sim 50\%$  compared with that of monolayer. Based on the above discussion, the larger the bonding length, the larger the negative Poisson's ratio. Compared to the bond length  $r_{12}$ , the bond length  $r_{34}$  is almost parallel to the  $z$  direction, which is directly related to the negative Poisson's ratio. Due to the interlayer vdW interaction introduced by an additional layer,  $r_{34}$  is increased to be 2.54 Å, resulting in a larger negative Poisson's ratio in bilayer.

In the case of trilayer, as shown in Fig. 3(b), the stress-strain curves  $L_1$  and  $L_3$  are identical, leaving the curve  $L_2$  deviated from  $L_1$  and  $L_3$  in the whole stress range. All these coincide with the symmetry of trilayer where layers  $L_1$  and  $L_3$  are symmetrically equivalent, but not for layer  $L_2$ . This leads to two negative Poisson's ratios. One is about -0.13 for the layers  $L_1$  and  $L_3$ . The other one is about -0.098 for the layer  $L_2$ , which is smaller than those of  $L_1$  and  $L_3$ . This is because the length  $r_{34}$  of layer  $L_2$  is 2.51 Å, which is smaller than the value of 2.55 Å for layers  $L_1$  and  $L_3$ . When any more layer is added, the internal bond lengths in particular  $r_{34}$  will be not changed largely. For example, in the case of four-layer, the bond lengths  $r_{34}$  are 2.55 Å and 2.54 Å for  $L_1$  (or  $L_4$ ) and  $L_2$  (or  $L_3$ ), which are very close to the value of 2.55 Å in the bulk arsenic. The obtained negative Poisson ratio of four-layer is about -0.121 (averaged value), as shown in Fig. 3(c). This value approaches the bulk's value of -0.125, as shown in Fig. 3(d). This means that the quantum effect on the negative Poisson's ratios is limited within four layers.

To further understand the layer stacking on the negative Poisson's ratios, we demonstrate it from the intrinsic puckered structure combined with the associated stress-strain curves  $\varepsilon_x$  versus  $\varepsilon_y$ . As pointed out above, the hinge-like structure is the origin of the negative Poisson's ratios in few-layer arsenic. The reason is as follows. When few-layer arsenic is stretched in the  $y$  direction, the layer contracts in the  $x$  direction, protected by the normal Poisson's ratios, as shown in Figs. 1(c) and 4(a)-4(d). In other words, atoms 3 and 4 as well as atoms 1 and 6 move inward along the  $x$  direction when stretched in the  $y$  direction (see Fig. 1(a)). This directly causes the bond angles  $\theta_{234}$  and  $\theta_{216}$  smaller compared to the initial values. Taking into account all the values of  $\theta_{234}$  and  $\theta_{216}$  (with/without strain) being larger than  $90^\circ$ , the layer thickness along the  $z$  direction (the projected distance of  $r_{34}$  or  $r_{16}$ ) is increased, leading to a negative Poisson's ratio. Therefore, the bond angles  $\theta_{234}$  and  $\theta_{216}$  being larger than  $90^\circ$  is another necessary condition for the negative Poisson's ratios

in few-layer arsenic. This is also true for BP as the bond angle  $\theta_{234}$  is  $97.64^\circ$  in BP [12]. If a material possesses the bond angles  $\theta_{234}$  and  $\theta_{216}$  being smaller than  $90^\circ$ , the negative Poisson's ratio will disappear. Future researches can test this prediction.

Due to the layer stacking, the normal Poisson's ratios are increased from 1.07 at monolayer (Fig. 1(c)) to 1.19 at four-layer (Fig. 4(c)). This implies that the decrease of  $\theta_{234}$  or  $\theta_{216}$  under the same stretching in the  $y$  direction is enhanced as layer increases. As a result, the negative Poisson's ratio increases with layer. For four-layer arsenic, the normal Poisson's ratio is very close to the bulk's value (Figs. 4(c) and 4(d)). This is the reason why the negative Poisson's ratio can approach the bulk's limit at four-layer. This tells us that the effect of layer stacking goes into the negative Poisson's ratio in the  $y$  direction which is indeed through the normal Poisson's ratio in the  $x$  direction.

In conclusion, the negative Poisson's ratio is for the first time reported in few-layer arsenic through using first-principles calculations. The magnitude of negative Poisson's ratio is about 0.1 at monolayer, which is about five times of magnitude larger than that of monolayer BP, suggesting extended applications in those special areas such as defence and medicine. When layer increases, the negative Poisson's ratio become large (more negative). The limited value of around -0.12 is predicted at four-layer, which is very close to the bulk's value. The underlying mechanism is demonstrated based on the layer-dependent internal bond length  $r_{34}$  and the normal Poisson's ratio of  $\varepsilon_x$  versus  $\varepsilon_y$ . The study like ours sheds new light on the layer-dependent negative Poisson's ratio in those hinge-like vdW nano-materials, which will evolve into an active field.

This work was supported by the National Basic Research Program of China under Grant No. 2012CB933101 and the National Science Foundation under Grant No. 51372107, No. 11104122 and No. 51202099. This work was also supported by the National Science Foundation for Fostering Talents in Basic Research of the National Natural Science Foundation of China. We also acknowledge this work as done on Lanzhou University's high-performance computer Fermi.

\*Email: sims@lzu.edu.cn

†Email: xueds@lzu.edu.cn

---

[1] L. J. Gibson, K. E. Easterling, and M. F. Ashby, Proc. R. Soc. London Ser. A **377**, 99 (1981).

- [2] R. S. Lakes, *Science* **235**, 1038 (1987).
- [3] G. N. Greaves, A. L. Greer, R. S. Lakes, and T. Rouxel, *Nature Mater.* **10**, 823 (2011).
- [4] A. Y. Haeri, D. J. Weidner, and J. B. Parise, *Science* **257**, 650 (1992).
- [5] D. J. Gunton and G. A. Saunders, *J. Mater. Sci.* **7**, 1061 (1972).
- [6] G. Milton, *J. Mech. Phys. Solids* **40**, 1105 (1992).
- [7] Q. Liu, *Literature Review: Materials with Negative Poisson's Ratios and Potential Applications to Aerospace and Defence*, (DSTO, Defence Science and Technology Organisation, 2006).
- [8] K. E. Evans and K. L. Alderson, *Adv. Mater.* **12**, 617 (2000).
- [9] L. J. Hall, V. R. Coluci, D. S. Galvão, M. E. Kozlov, M. Zhang, S. O. Dantas, and R. H. Baughman, *Science* **320**, 504 (2008).
- [10] G. Grimvall, *Thermophysical Properties of Materials*, (North-Holland, Amsterdam, 1986).
- [11] N. R. Keskar and J. R. Chelikowsky, *Nature* **358**, 222 (1992).
- [12] J.-W. Jiang and H. S. Park, *Nat. Commun.* **5**, 4727 (2014).
- [13] Z. Y. Zhang *et al.* arXiv:1411.3165.
- [14] C. Kamal and M. Ezawa, arXiv:1410.5166.
- [15] J. M. Soler, E. Artacho, J. Gale, A. García, J. Junquera, P. Ordejón, and D. Sánchez-Portal, *J. Phys.: Condens. Matter* **14**, 2745 (2002).
- [16] J. P. Perdew, K. Burke, and M. Ernzerhof, *Phys. Rev. Lett.* **77**, 3865 (1996).
- [17] V. R. Cooper, *Phys. Rev. B* **81**, 161104(R) (2010).
- [18] N. Troullier and J. L. Martins, *Phys. Rev. B* **43**, 1993 (1991).
- [19] L. Kleinman and D. M. Bylander, *Phys. Rev. Lett.* **48**, 1425 (1982).
- [20] E. Artacho, D. Sánchez-Portal, P. Ordejón, A. García, and J. M. Soler, *Phys. Status Solidi B* **215**, 809 (1999).
- [21] P. M. Smith, A. J. Leadbetter, and A. J. Apling, *Philos. Mag. B* **31**, 57 (1975).
- [22] C. Kittel, *Introduction to Solid State Physics*, eighth ed. (Wiley, Hoboken, NJ, 2004).
- [23] A. K. Geim and I. V. Grigorieva, *Nature* **499**, 419 (2013).

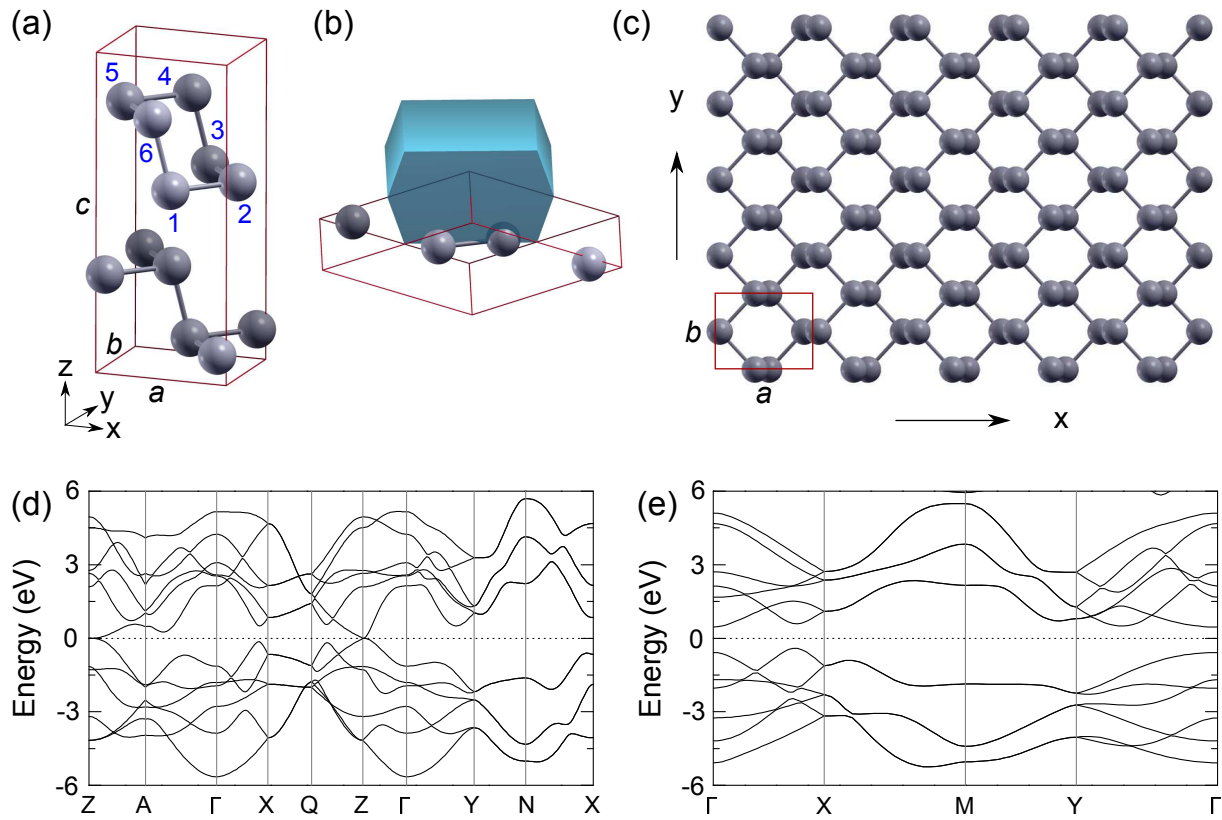


FIG. 1: (color online). (a) Conventional unit cell of orthorhombic arsenic with lattice constants  $a$ ,  $b$ , and  $c$  and internal atoms 1-6. (b) Primitive unit cell and its Wigner-Seitz cell (blue shaded configuration). (c) Top view of monolayer arsenic with rectangle showing the unit cell. Band structures of (d) bulk and (e) monolayer.

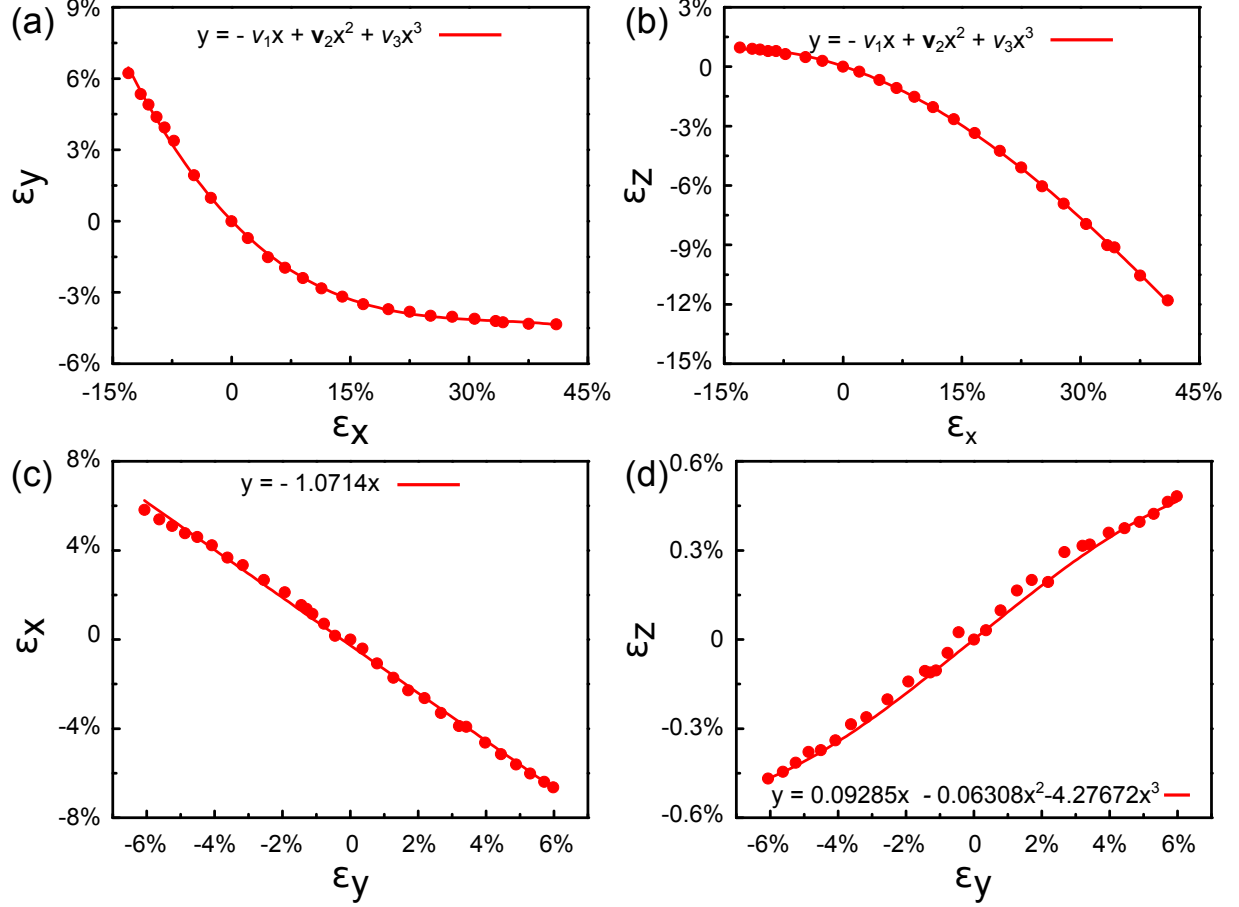


FIG. 2: (a)  $\varepsilon_y$  versus  $\varepsilon_x$ . The solid circles are simulated data and the line is fitted by function  $y = -\nu_1 x + \nu_2 x^2 + \nu_3 x^3$ , with  $\nu_1 = 0.35$  as the linear Poisson ratio,  $\nu_2 = 1.00$  and  $\nu_3 = -1.00$ . (b)  $\varepsilon_z$  versus  $\varepsilon_x$ . The fitted linear Poisson ratio is obtained to  $\nu_1 = 0.13$ , as well as  $\nu_2 = -0.48$  and  $\nu_3 = 0.23$ . (c)  $\varepsilon_x$  versus  $\varepsilon_y$ . Data are fitted to function  $y = -\nu x$ , with  $\nu = 1.07$  as the linear Poisson ratio. (d)  $\varepsilon_z$  versus  $\varepsilon_y$ . Data are fitted to function  $y = -\nu_1 x + \nu_3 x^3$ , with the negative Poisson ratio  $\nu = \nu_1 = -0.093$ .

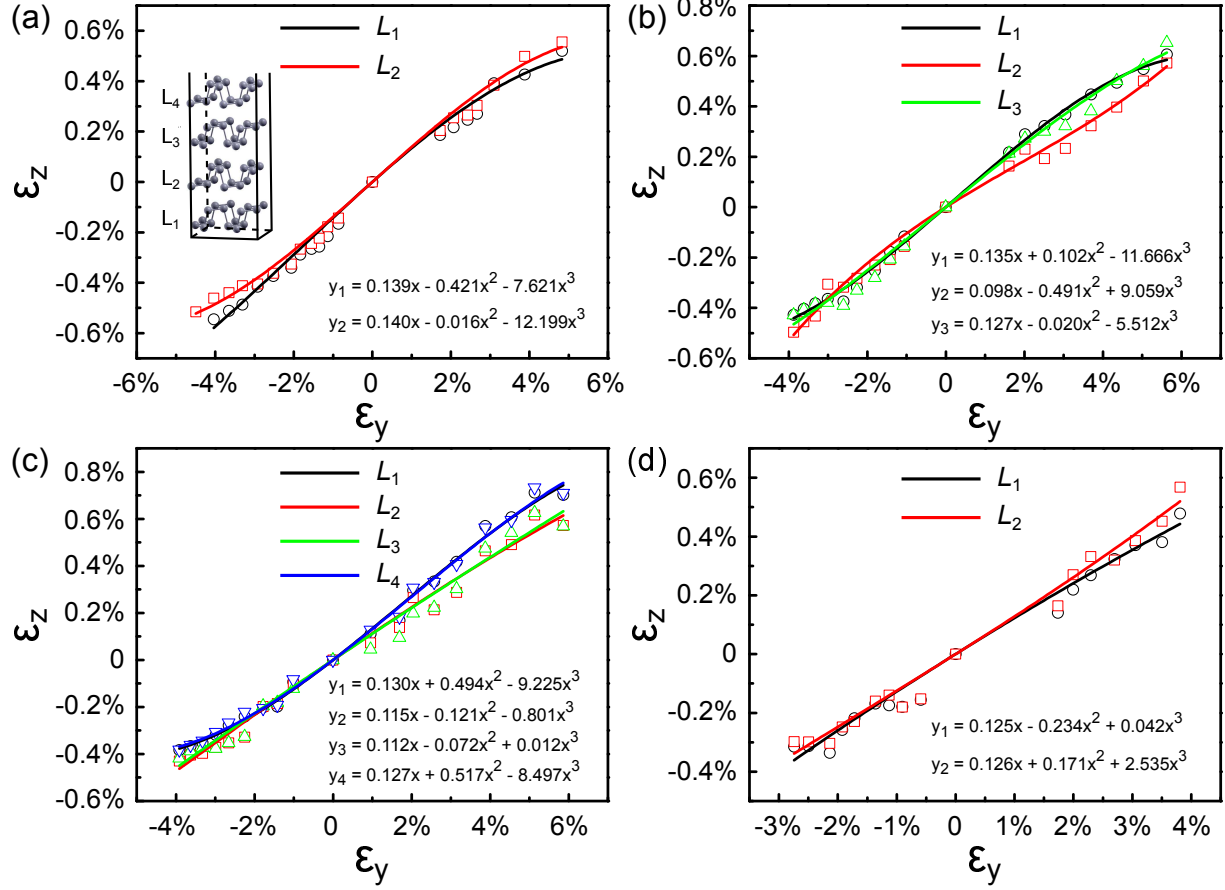


FIG. 3: (color online). (a)  $\varepsilon_z$  versus  $\varepsilon_y$  for bilayer arsenic. Inset shows a four-layer arsenic with layers labeled as  $L_1 - L_4$  from bottom to top. The fitted functions for each layer are given as well.  $\varepsilon_z$  versus  $\varepsilon_y$  for (b) trilayer, (c) four-layer and (d) bulk arsenic. Other denotes are the same as in (a).

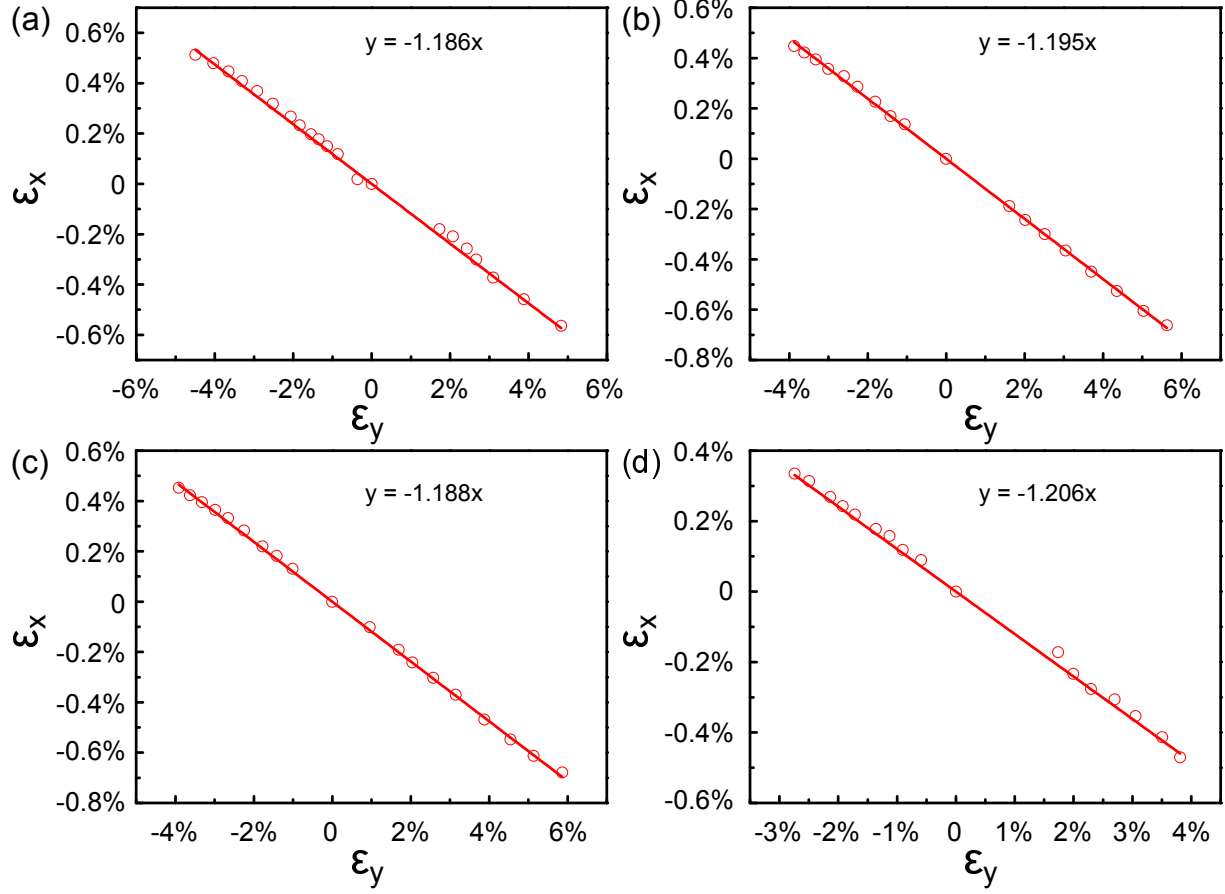


FIG. 4:  $\varepsilon_x$  versus  $\varepsilon_y$  for (a) bilayer, (b) trilayer, (c) four-layer and (d) bulk arsenic. The fitted functions are also given.